Remote Sensing of Environment 152 (2014) 270–278

Contents lists available at ScienceDirect

Remote Sensing of Environment

journal homepage: www.elsevier.com/locate/rse

Satellite remote sensing reveals coastal upwelling events in the San Matías Gulf—Northern Patagonia

Juan P. Pisoni [a,*], Andrés L. Rivas [b], Alberto R. Piola [c]

[a] Centro Nacional Patagónico (CENPAT-CONICET), Argentina
[b] Centro Nacional Patagónico (CENPAT-CONICET) and Fac. Cs. Naturales (UNPSJB), Argentina
[c] Servicio de Hidrografía Naval, Universidad de Buenos Aires and Instituto Franco-Argentino sobre Estudios del Clima y sus Impactos (CONICET), Argentina

ARTICLE INFO

Article history:
Received 27 November 2013
Received in revised form 1 June 2014
Accepted 28 June 2014
Available online xxxx

Keywords:
Coastal upwelling events
Wind impulse
San Matías gulf
SST images

ABSTRACT

Coastal upwelling events are effective in fluxing nutrients upward to the euphotic layer, thus promoting the growth of marine phytoplankton. Satellite data may provide useful information to detect and characterize upwelling events in regions of sparse in-situ observations. We analyze the coastal upwelling process on the western San Matías Gulf, on the northern continental shelf of Argentina, based on the analysis of remote sensing and in-situ data. Upwelling events are characterized by their frequency of occurrence and magnitude. During the austral summer we found roughly 6 upwelling-favorable wind events per year. Satellite derived sea surface temperature (SST) data provide evidence of upwelling in 85% of the cases between 2000 and 2008. Analysis of specific events provides clues on the wind forcing characteristics required to generate upwelling, and on characteristic space and time scales of the process. On February 2005 SST data reveal a narrow coastal band (~10 km) of relative cold water extending ~100 km along the west coast of SMG. The SST in this band was 1.5 °C lower than further offshore. Near bottom temperature fluctuations from in-situ daily observations collected at two near-shore locations are significantly correlated with along-shore wind stress, suggesting that coastal upwelling is a dominant process controlling high-frequency temperature fluctuations near-shore. A simple quantitative estimate reveals a volume of upwelled water reaching the sea surface of about 10^{10} m^3 during one relatively intense upwelling event.

1. Introduction

The Patagonia Continental Shelf (PCS) in the southwestern South Atlantic presents high phytoplankton biomass (e.g. Garcia et al., 2008; Lutz et al., 2010; Rivas, Dogliotti, & Gagliardini, 2006; Romero, Piola, Charo, & Eiras Garcia, 2006) which spreads up the marine food web reaching top predators and significant fisheries (Acha, Mianzan, Guerrero, Favero, & Bava, 2004). This high productivity is promoted by vertical nutrient fluxes by strong vertical mixing induced by winds and near-shore tidal flows, and shelf break upwelling (Matano & Palma, 2008; Matano, Palma, & Piola, 2010; Palma, Matano, & Piola, 2008). In contrast with these productive regions, some deep near-shore locations without strong tidal stirring, present relatively low primary production. Such is the case of the San Matías Gulf (SMG), the second largest gulf in the Argentine Patagonia, where tidal mixing within the gulf is not sufficiently intense to fertilize the surface layer, because it is considerably deeper than the adjacent PCS (200 m vs 70 m). Interestingly, however, the SMG is recognized for important fishing activities (Ocampo-Reinaldo et al., 2013), with total landings exceeding 10^4 t/year (González, Narvarte, & Morsan, 2004). The SMG productivity is thought to be sustained by the supply of nutrients from the lower layers and the entrance of nutrient-rich waters from the exterior shelf (Sabatini & Martos, 2002), with negligible atmospheric and continental contributions (Carreto, Verona, Casal, & Laborde, 1974). Tidal energy dissipation at mouth and over the adjacent PCS (Glorioso & Flather, 1995; Palma, Matano, & Piola, 2004; Tonini, Palma, & Piola, 2013) generates tidal fronts (Bava, Gagliardini, Dogliotti, & Lasta, 2002; Rivas & Pisoni, 2010) where the coexistence of stratified and mixed waters maintains high biological productivity. Williams (2004) analyzed the availability of macronutrients and the relationship between primary and secondary productivity in the SMG, and suggested that coastal upwelling may be required to close the nutrient balance. Based on the analysis of a high resolution numerical model Tonini (2010) observed upwelling (downwelling) along the ~140 km west coast of SMG in response to northerly (southerly) winds.

Upwelling processes carry subsurface, nutrient-rich waters to the upper layer generally leading to high biological productivity. Coastal upwelling along mid-latitude eastern boundaries sustains the most significant global fisheries (e.g. Bakun, 1990; Beardsley, Dorman, Friehe, Rosenfeld, & Winnant, 1987; Calvert & Price, 1971; Ryther, 1969). In addition to major upwelling systems several other small-scale coastal

* Corresponding author at: Centro Nacional Patagónico (Consejo Nacional de Investigaciones Científicas y Técnicas de Argentina)—Bvd. Brown 2915 (U9120ACF), Puerto Madryn, Argentina. Tel.: +54 280 451024.
E-mail address: pisoni@cenpat.edu.ar (J.P. Pisoni).

http://dx.doi.org/10.1016/j.rse.2014.06.019
0034-4257/

upwelling regions are well-documented, such as Nova Scotia (Petrie, Topliss, & Wright, 1987), the China Sea (Kuo, Zheng, & Ho, 2000), Galicia (Torres, Barton, Miller, & Fanjul, 2003), North Carolina (Forde, 2005), Cabo Frio (Castelao & Barth, 2006), the Baltic Sea (Fennel, Radtke, Schmidt, & Neumann, 2010), and the Sea of Japan (Park & Kim, 2010), among others. Recently, sporadic upwelling has been reported along the west coast of Australia (Rossi, Feng, Pattiaratchi, Roughan, & Waite, 2013).

The upwelling intensity and, ultimately the nutrient flux and its biological impact are determined primarily by the direction, magnitude and persistence of the wind relative to the coast. Csanady (1977) defined the impulse (I) as the time integral of along-shore wind stress and found that a minimum impulse is necessary to develop a full upwelling (when the thermocline intersects the surface) in a two-layer fluid. The magnitude of the required wind stress impulse is proportional to the product of top layer depth and propagation velocity of long-waves on the thermocline. The effects of along-shore wind impulse remain until destroyed by friction. Haapala (1994) showed that a short-duration and weak intensity wind in the Gulf of Finland is enough to produce upwelling when the water column is vertically stable. In this case, the wind acts over the layer above the thermocline (mixed layer depth). For a homogeneous water column, the wind influence penetrates deeper and more energy is needed to produce coastal upwelling. Lentz and Chapman (2004) conclude that with a gentle bottom slope and reduced vertical stability bottom friction is able to balance the wind stress, the offshore flow is weak and the onshore flow is bounded (confined) to the bottom layer. On the contrary, with a strong stratification and a steep slope, onshore flow is intense and extends from the bottom to the base of the thermocline.

Despite the biological significance of upwelling, most coastal regions around the world lack in-situ observations with enough space–time resolution to detect and analyze episodic events associated with high-frequency wind fluctuations. For instance, though numerical simulations predict upwelling along the west coast of SMG in response to northerly winds (e.g. Tonini, 2010; Tonini & Palma, 2011), these events have not been confirmed by observations. The lack of observations may be intrinsic to the short-term and sporadic nature of wind driven upwelling as well as to the scarcity of in-situ data. The combined analysis of satellite based wind, infrared and/or visible satellite data may partially overcome these difficulties. In summer, upwelling events can be identified as along-shore bands of low sea surface temperature (SST) and high chlorophyll concentration. Though relatively low SST can also result from intensified vertical mixing in regions of high tidal dissipation, numerical simulations suggest that tidal mixing is not particularly intense along the western boundary of SMG (Glorioso & Flather, 1995; Palma et al., 2004; Tonini et al., 2013). The lack of observations of along-shore thermal fronts in summer, which are characteristic of strong tidal dissipation (e.g. Bava et al., 2002; Rivas & Pisoni, 2010; Romero et al., 2006) confirms the modeling results. Thus, we hypothesize that observations of relatively low SST near-shore are indicative of coastal upwelling. The main goals of this study are: to verify the existence of upwelling events along the west coast of SMG, to characterize the conditions that lead to coastal upwelling, and to analyze their spatial scale and frequency of occurrence. Thus, the combined analysis of satellite derived sea surface temperature and surface winds proposed herein is a relevant aspect of this study, which can be applied to other data sparse regions.

The paper is organized as follows. The data and methods are presented in Section 2. Section 3 describes the conditions required to produce upwelling along the west coast of SMG and their frequency of occurrence. In Section 4 specific upwelling events are analyzed and the results are discussed in Section 5.

2. Data and methods

The study includes the analysis of satellite derived SST, color and wind data. In-situ observations of wind at two coastal stations and an ocean mooring and two ocean temperature time series are used to verify the quality of the satellite data and/or the occurrence of an upwelling event.

The satellite SST data were obtained from the Advance Very High Resolution Radiometer (AVHRR, 1.1 × 1.1 km resolution) onboard the NOAA-12 to NOAA-18 satellites and span 9 years from January 2000 to December 2008. Ocean color data are obtained from MODIS/Aqua at 1.1 × 1.1 km resolution. Details about the images processing are described in Williams et al. (2013).

Wind data are derived from the QuikSCAT scatterometer (www.remss.com) for the period 2000–2008. Since the SMG is relatively small compared to the spatial scale of synoptic weather systems, 9 nodes satellite wind data located in the SMG were averaged (Figs. 1 and 4). Also, historical surface wind from NCEP reanalysis (Kalnay et al., 1996) for the first days of May 1971 on two nodes near the mouth of SMG was used.

The near-shore temperature time series are from two bottom mounted thermistors (ONSET, TidBit v2-UTBI-001, ±0.20 °C) installed on the western coast of SMG (El Sótano, ES and Punta Pozos, PP, see Fig. 1). The thermistors recorded the temperature at 6 h intervals during eleven months from austral spring 2007 to late winter 2008 (Table 1).

A surface buoy in the northwestern of the SMG provided wind data at 3 m above sea level (Table 1). This data were used to estimate the wind velocity at 10 m using the expression of Wood, Roughan, and Tate (2012). Additional wind data from two coastal stations located in San Antonio Oeste and Puerto Madryn (Fig. 1) were analyzed. Fig. 2 shows the seasonal characteristics of the wind from QuikSCAT data (2000–2008 period) using the average of the 9 nodes shown in Fig. 1. The QuikSCAT wind statistics reveal higher frequency of northwesterly winds in autumn–winter, increasing the frequency from the east in spring–summer, probably due to the sea breeze which is ubiquitous at nearby coastal locations (e.g. Dellatorre, Pisoni, Barón, & Rivas, 2012), and relatively high percentage of northerly winds throughout the year. These wind patterns are in agreement with those described by Lucas, Guerrero, Mianzan, Acha, and Lasta (2005) who analyzed coastal stations, and also coincide with the wind climatology from San Antonio Oeste meteorological station (see Fig. 1) (SMN, 1958, 1963, 1981, 1986). The wind climatology from Puerto Madryn (located ~225 km south of San Antonio Oeste, Fig. 1) also indicates a decrease in northerly wind frequency from winter to summer consistent with the increase in the summer breeze, although with a much greater frequency of southwesterly winds (not shown). The quality of the wind data derived from QuikSCAT is determined by the high correlation ($r = 0.91$) with in-situ wind data from the ocean buoy (see Fig. 1 and Table 1) estimated using 12-hourly observations from July to December 2005.

Because QuikSCAT winds are in good agreement with coastal winds, the former were used to identify periods of upwelling. Different criteria for the identification of coastal upwelling conditions based on the duration and magnitude of the wind were tested. In this work we use I, as defined by Csanady (1977), by integrating the negative (northerly) along-shore wind stress. Coastal upwelling events were considered when $I < -10^4$ kg m^{-1} s^{-1}, which is equivalent to northerly wind of ~9 m s^{-1} during 1 day (~6.3 m s^{-1} during 2 days or of 5.2 m s^{-1} during 3 days). In addition, events are considered distinct from each other if the southerly along-shore wind blows during at least one day.

3. Quantification of upwelling events

The number of upwelling-favorable wind events detected from January 2000 to December 2008 is shown in Fig. 3. During the summer (1092 days between December and March, for the 9-year period), when satellite images display relatively cold waters along the SMG west coast, there were a total of 56 events of upwelling-favorable winds, according to the adopted impulse criterion (Fig. 3). For some events more than

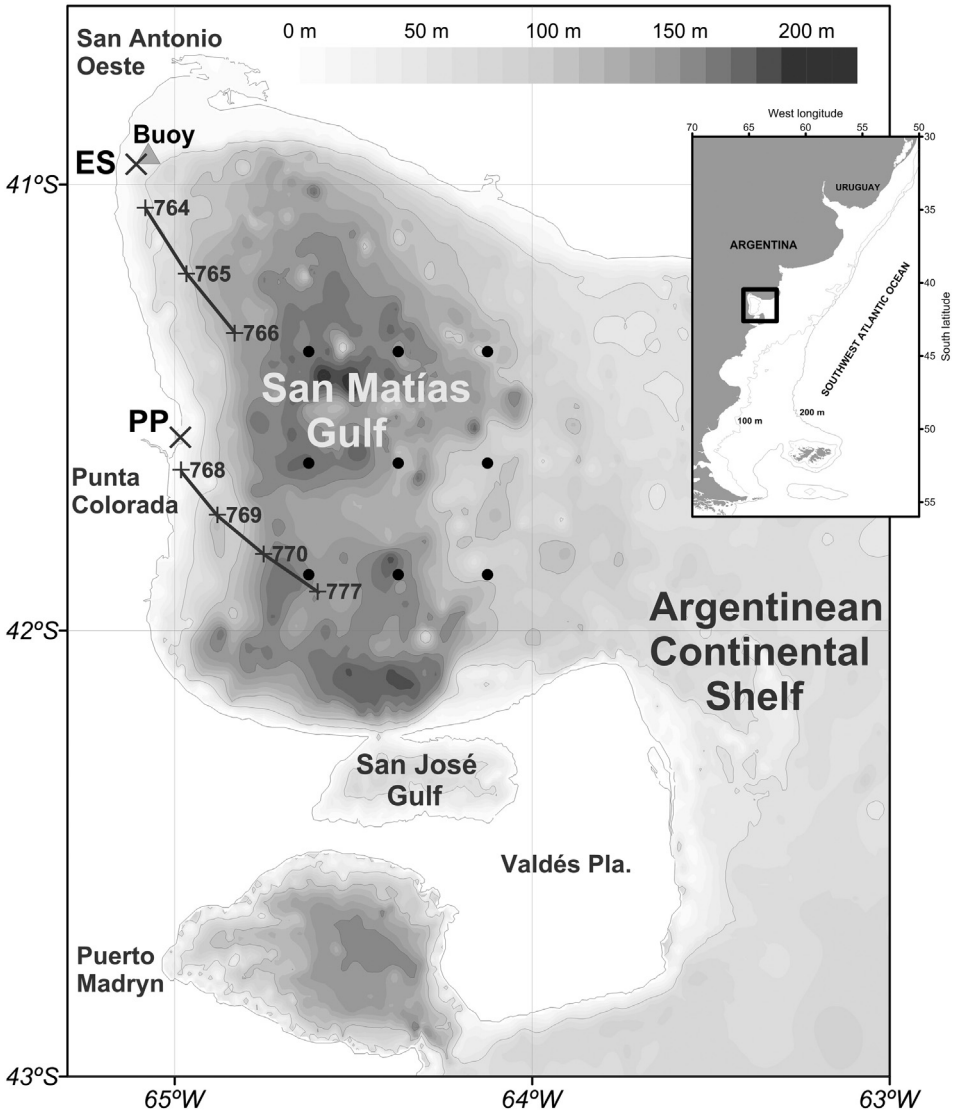

Fig. 1. Locations of in-situ temperature observations: buoy (triangle), El Sótano (ES) and Punta Pozos (PP) (crosses). Lines and crosses indicate location of hydrographic stations occupied in December 2006. Dots represent QuikSCAT nodes. Shading represents the bathymetry (m).

one SST image is available, while for 17 events cloud cover prevented the use of the images. Thirty nine coastal upwelling events were studied based on the analysis multiple quasi-simultaneous (within 1–2 days) SST images. Relatively low SSTs along the west coast of SMG were associated with 33 out of these 39 events. This is roughly equivalent to 85% of the cases and supports the adopted wind impulse criterion.

Table 1
Sampling periods, positions and depths of temperature sensors ES and PP at low tide and the oceanic buoy (see Fig. 1 for locations). The averaged tidal amplitude (m) is given in parenthesis in the Depth column. Depths were estimated from nautical charts. Depth variations are the height mean tide at San Antonio Oeste and Punta Colorada (see Fig. 1) according to tidal prediction tables (SHN, 2011).

	Period (d/m/y)	Location		Depth
Buoy	4/7/2005 to 19/12/2005	40° 56.28′ S	65° 4.44′ W	~20 m
El Sótano (ES)	7/9/2007 to 26/8/2008	40° 57.27′ S	65° 6.46′ W	15 m (+6.54)
Pta. Pozos (PP)	3/10/2007 to 7/9/2008	41° 34.01′ S	64° 59.03′ W	5 m (+5.96)

4. Specific upwelling events

4.1. February 2005

A particularly intense upwelling event in the west coast of SMG was observed in early February 2005. Satellite derived SST and chlorophyll as observed on 4 February 2005 are shown in Fig. 4. The SST image presents a large pool of warm waters (SST > 21 °C) in the northern SMG and a tongue of cold water (SST < 17 °C) intruding from the neighboring continental shelf along the southern coast of SMG (Fig. 4a). The southern portions of the SMG are relatively cold compared to the north, with SST ~ 18 °C. This pattern is characteristic of the summer conditions (Gagliardini & Rivas, 2004; Piola & Scasso, 1988; Tonini et al., 2013; Williams et al., 2013). In addition, a narrow band (~10 km) of relatively cold water is observed along the west coast, with SST ~ 16.5 °C south of 41.5°S and <19 °C further north. On average, the surface waters along the west coast are about 1.5 °C colder than further offshore. The band of cold surface waters, indicative of upwelling, extends along the coast for over 100 km.

The amount of sunlight and stratification available in summer favor the growth of phytoplankton. However, the productivity is frequently

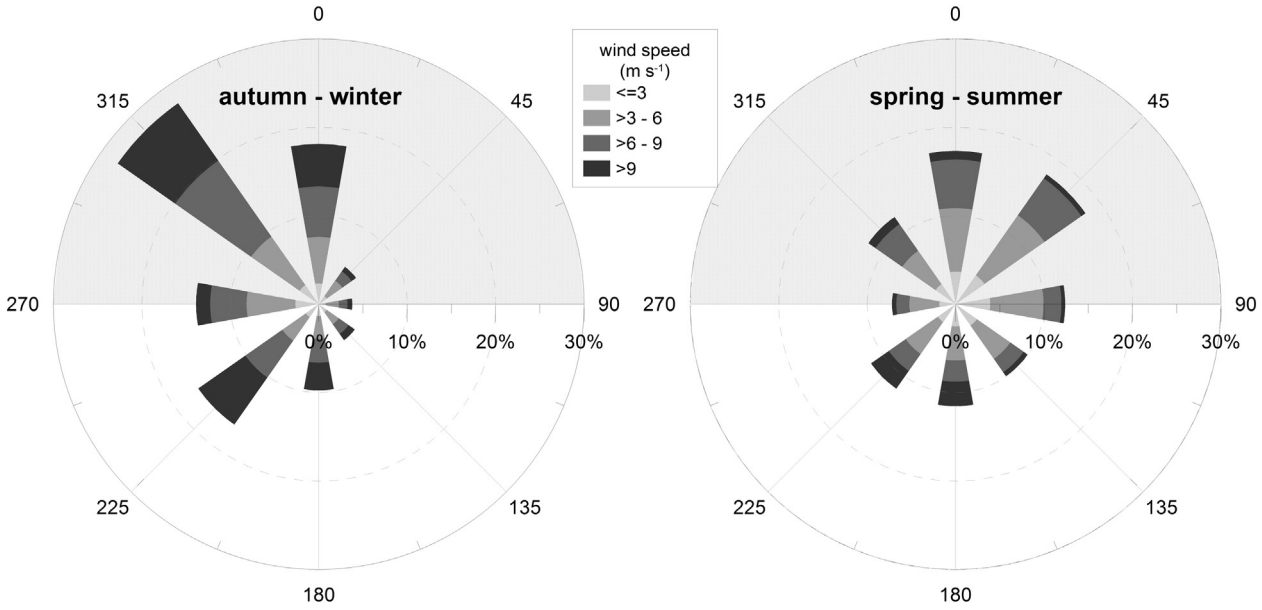

Fig. 2. QuikSCAT climatological wind statistics 2000–2008 on SMG. The radial bar indicates the direction from which the wind blows and the bar length the relative frequency from each quadrant. The shaded area represents the direction of upwelling-favorable wind.

limited by low nutrient concentrations in the upper layer, which are consumed during the spring bloom, except close to ocean fronts (e.g. Carreto, Lutz, Carignan, Colleoni, & Marcos, 1995). Consequently, vertical nutrient fluxes associated with coastal upwelling may have a particularly strong biological impact in summer. The surface chlorophyll concentration (Fig. 4b) is relatively low in most of the northern gulf (~0.5 mg m^{-3}) and, away from the coast is somewhat higher in the southern domain (~1 mg m^{-3}, Fig. 4b). In contrast, the narrow coastal band where cold waters are observed, particularly south of 41.5 °S, is associated with relatively high surface chlorophyll (>2 mg m^{-3}). Nevertheless, the maximum values of chlorophyll in the southeast of Fig. 4b are probably due to high concentrations of sediments located in a high turbulence zone associated with strong tidal dissipation at that location (Palma et al., 2004). It is important to note that though most upwelling events in the SMG identified by our wind impulse criterion present low SST (see Section 3), some events are not associated with high surface chlorophyll. This is not too surprising as the biological response to upwelling may be modulated by several other factors such as vertical stratification, nutrient concentration in the lower layer and grazing, among others.

To evaluate the evolution of SST across the upwelling front during this event, we analyze a cross-shore SST transect on 41.6 °S spanning about 18 km from shore (Fig. 4a). The SST data are from NOAA-12 satellite between 1 and 5 February 2005. The first available cloud free image prior to 1 February, collected on 26 January is also presented as reference. To minimize the effect of pixel to pixel noise frequently observed in high resolution SST data, temperatures were averaged over 3 pixels in the along-shore direction. During the first 5 days of February, relatively low temperatures are present along the coast, and cross-shore SST differences of ~2 °C are observed. The coastal band of relatively cold waters appears to widen until 4 February, reaching ~10 km offshore, but on 5 February the band narrows as the front displaces onshore (Fig. 5). The strong warm SST near-shore observed on 4 February, and to a lesser extent in other sections, is probably due to coastal contamination of the SST data. The time evolution of the negative along-shore wind stress between 25 January and 9 February 2005 is shown in Fig. 6. On 1 February the along-shore wind speed reversed from southerly (6 m s^{-1}) to northerly (7 m s^{-1}) and continued blowing from that direction with a decreasing intensity until 8 February (Fig. 6). Thus, the offshore displacement of the upwelling front (1–4 February, Fig. 5) occurs at the time of substantial increase of southward wind impulse (Fig. 6), whereas the onshore displacement on 5 February occurs during the time the wind impulse stabilizes. Based on the analysis of a two-layer model Csanady (1997) concluded that the offshore displacement of the upwelling front is proportional to the excess of I and inversely proportional to the mixed layer depth. As on 5 February I continues increasing despite the reduction of along-shore wind stress, this simple model predicts that the mixed layer depth should also continue increasing.

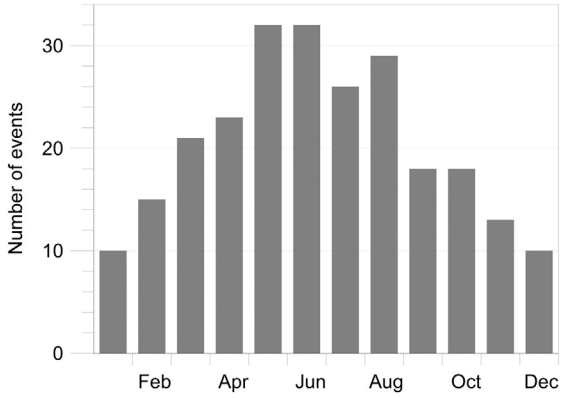

Fig. 3. Number of upwelling events between 2000 and 2008 based on the along-shore wind impulse $< -10^4$ kg m^{-1} s^{-1}.

The offshore transport in the Ekman layer, which must be balanced by coastal upwelling, leads to lower SST along the coastal band, and presumably enhances the nutrient flux to the upper layer. Historical hydrographic data collected in SMG (e.g. Pisoni, 2012) and elsewhere in the SW Atlantic shelf (e.g. Carreto et al., 1995) suggest a tight temperature–nitrate relationship ($r^2 = 0.97$), with cold waters associated with high nutrient concentration. Our observations suggest that the coastal band of low SST and the high surface chlorophyll observed during the period of moderate northerly wind in early February 2005, are manifestations of a relatively intense wind driven upwelling event.

4.2. Events during 2007–2008

As mentioned above, bottom mounted temperature sensors were installed at two near-shore locations in the SMG from December 2007

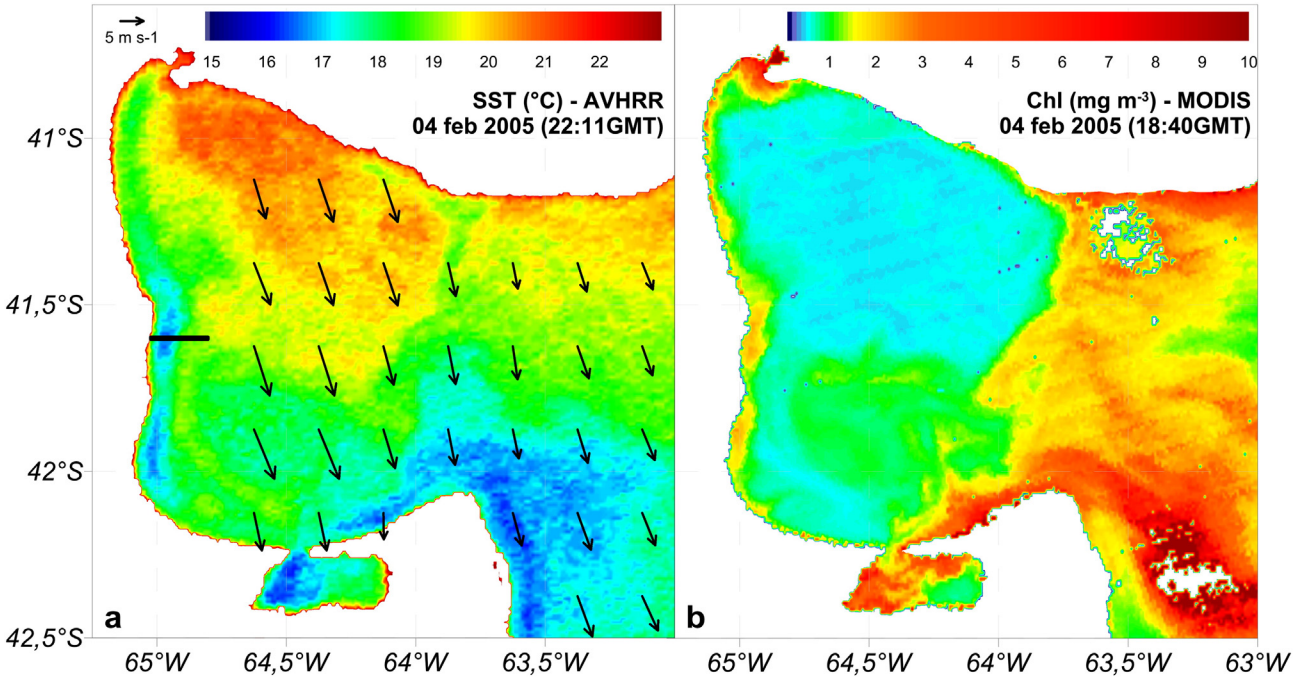

Fig. 4. (a) Sea surface temperature from AVHRR and (b) surface chlorophyll from MODIS/Aqua on 4 February 2005. The arrows in (a) represent the mean QuikSCAT wind velocity from 1 to 4 February, 2005. The black line indicates the location of the SST transect shown in Fig. 5.

to March 2008. Since these observations correspond to a period of strong stratification we expect that some of the temperature variability at these sites be correlated with the along-shore wind. Thus, we focus on the co-variability of temperature and along-shore winds. The analysis is based on the daily temperature changes $\Delta T/\Delta t$, where ΔT represents the temperature difference during the time-span of $\Delta t = 1$ day.

A day of intense northerly wind is sufficient to decrease the temperature in both thermistors almost immediately. However, bottom temperatures usually do not continue decreasing even if northerly winds remain. In turn, daily temperature changes suggest that the largest temperature decreases due to northerly winds are generally first observed at PP, located about 70 km south of ES.

Eight of the 56 upwelling-favorable wind events detected in the nine summers between 2000 and 2008 (see Fig. 3) occurred between December 2007 and March 2008 (Table 2). Thus, the number of wind events observed during that particular summer was higher than average.

The surface manifestation of these upwelling events is clear in satellite derived SST data. For example, the mean northerly (e.g. upwelling favorable) wind on 4 January 2008 was >8 m s^{-1} ($I_4 \sim -10^4$ kg m^{-1} s^{-1}, Table 2) and lead to a temperature decrease of 1.1 °C at PP during that day and of 1.75 °C the following day, when $I_5 = -1.07 \times 10^4$ kg m^{-1} s^{-1}. On 5 January the temperature recorded at ES decreased 0.75 °C (0.96 °C in two days, Table 2). The satellite derived SST distribution on 5 January displays two small (~15 km) pockets of cold waters near the western coast of SMG south of PP (SST < 16.5 °C in Fig. 7a). The SST at these two locations is ~1.5 °C lower than further offshore (Fig. 7a). An additional event of strong northerly wind (>10 m s^{-1}) was observed on 18 March 2008 ($I_{18} = -1.4 \times 10^4$ kg m^{-1} s^{-1}, Table 2). This event led to a bottom temperature decrease of around 0.6 °C on both thermistors during the following day, when $I_{19} = -1.6 \times 10^4$ kg m^{-1} s^{-1}. On 19 March the satellite derived SST distribution displays a cold coastal band (SST < 18.5 °C in Fig. 7b), where the SST in both, the northern and southern regions, was 0.5 °C lower than offshore. The upwelling during 5 January leads to lower SST south of about 41.5 °S (Fig. 7a). This meridional difference may be associated with the deepening of the thermocline in the northern SMG, which is in turn associated with the relatively intense cyclonic circulation observed in that region (Piola & Scasso, 1988; Tonini et al., 2013). In contrast with the January situation, on 19 March, the cold band of SST extends northward along the west coast beyond 41 °S. This difference in the meridional extension of the cold SST band is probably caused by a weakening of the thermocline in March and by the greater wind impulse observed at that time.

It is difficult to determine the precise duration of an upwelling event based on satellite SST data because cloud coverage frequently obscures the timing of the onset or decay of a particular event. On the other hand, based on the bottom temperature (T_{bottom}) observations we can make a rough estimate of the duration as the time elapsed between the time when T_{bottom} starts decreasing until it starts increasing. In the eight events detected between December 2007 and March 2008 based on the $I < -10^4$ kg m^{-1} s^{-1} criterion, T_{bottom} decreased (Table 2). Most of these events lasted ~2 days (Table 2). Additional cooling events during this period are also present, and though $I > -10^4$ kg m^{-1} s^{-1} in several cooling events, the wind was also upwelling favorable (not shown). None of the bottom cooling events observed during less intense northerly wind impulse is clearly associated with an extended band of cold anomalies along the coast. Given that the impulse threshold was adopted based on the observation of cold waters at the surface, the observation of subsurface cooling indicates that less intense northerly wind impulse may still cause upwelling that does not reach the surface and therefore does not manifest as a decrease of SST along the coast. In contrast, when southerly winds prevail (downwelling favorable) it is likely that the near bottom cooling is associated with northward advection of cold waters from the southern portions of the Gulf, intensification of tidal mixing near shore, and atmospheric forcing, among others.

The correlations between the cross-shore wind component and the bottom temperature variability at both sites are weak and negative during the warm period ($r < 0.05$, not statistically significant), suggesting no significant response to cross-shore wind variability. In contrast, the correlation between the along-shore wind and wind stress with bottom temperature variations at both sites is positive and statistically significant (between 0.18 and 0.42, $p < 0.01$), suggesting that northerly (southerly) wind decreases (increases) the bottom temperature. This last observation is in agreement with Ekman dynamics. Though

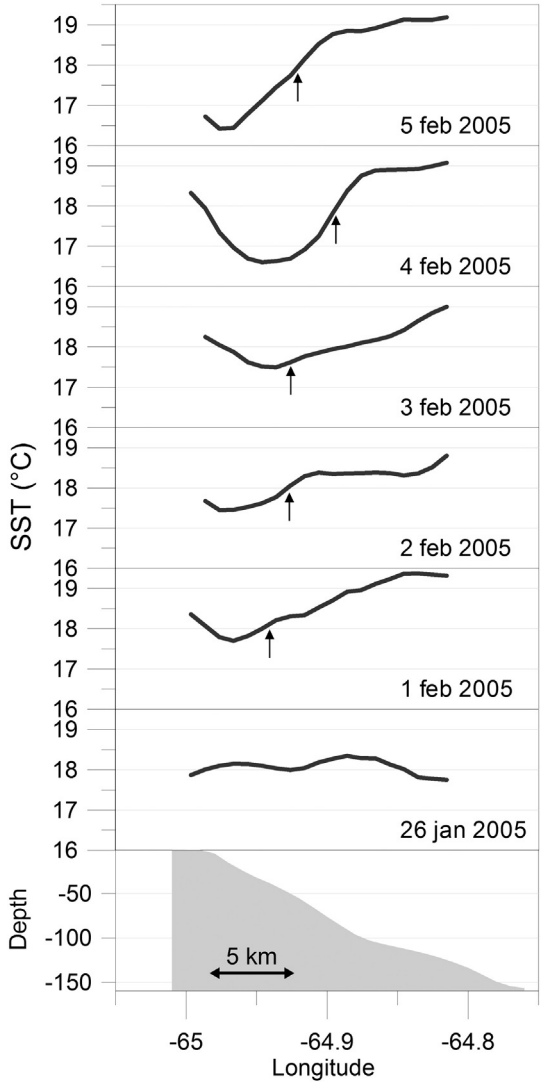

Fig. 5. SST and bathymetry (m, bottom panel) along the transect shown in Fig. 4a. The arrows indicate the location of the upwelling front.

offshore winds can cause upwelling along the inner-shelf during the stratified period (e.g. Tilburg, 2003), the magnitude of the correlation coefficients suggests that upwelling events are primarily caused by along-shore winds, in agreement with the observations of Csanady (1977).

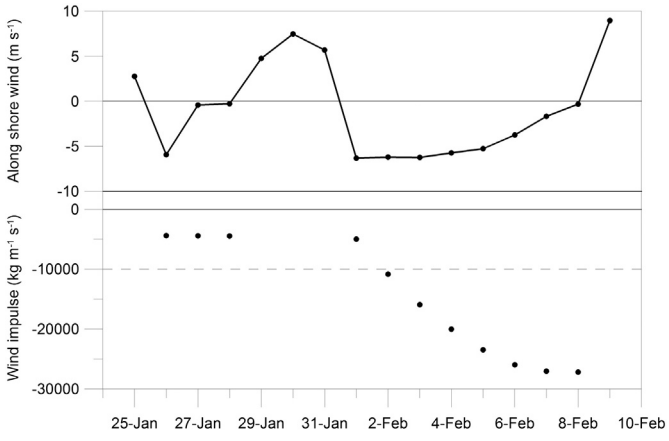

Fig. 6. Daily along-shore wind speed (upper panel) and along-shore wind impulse (bottom panel, only negative values shown) from QuikSCAT data. The dotted line in the lower panel (-10^4 kg m^{-1} s^{-1}) represents the impulse required to produce upwelling (see text).

4.3. Estimate of upwelling volume

Two hydrographic sections occupied across the western slope of SMG on 7 December 2006 (Fig. 1) are presented to further discuss the effects of northerly winds on the near-shore vertical stratification. On 6 December the wind speed was very low (~1.7 m s^{-1}) and northwesterly, while in the following day the wind turned to the north direction and increased beyond 9 m s^{-1}, producing $I = -10.9 \times 10^4$ kg m^{-1} s^{-1}. The northern section (Fig. 8a) was occupied early on the 7 December, while the southern section (Fig. 8b) was occupied at the end of that day. In the northern section, the isotherms deepen towards the coast, in response to the cyclonic circulation within the northern SMG (Piola & Scasso, 1988; Tonini et al., 2013). In contrast, in the southern section below 30 m depth the isotherms rise shoreward and the warm upper layer waters expand offshore. Thus, the temperature structure suggests the onset of upwelling (Fig. 8) without evidence of the development of a surface upwelling front. This is also confirmed from the analysis of SST images from 7 to 8 December, which show no evidence of cold waters along the western coast of SMG. Inspection of the vertical temperature distribution on the southern section indicates that a surface temperature drop large enough to produce a 1 °C temperature contrast between coastal and offshore waters requires upwelling from about 20 m depth.

Assuming $I = -10^4$ kg m^{-1} s^{-1} blowing over an ~100 km coastal band (L_y), the total volume of upwelled water is estimated as $I \cdot L_y / \rho \cdot f \sim 10^{10}$ m^3 (where ρ is the density of seawater and f is the local Coriolis parameter). This volume is ~0.6% of the total volume of the San Matías Gulf. Given that the cold coastal band is ~10 km wide (see Fig. 5) and assuming a northerly wind blowing during one-day, the required vertical velocity is ~10 m day^{-1}. The estimated vertical velocity is of the same order of magnitude of the near-bottom vertical velocity derived from a high resolution numerical model with realistic bottom topography forced by a northerly wind stress of 0.1 Pa (Tonini, 2010). This wind stress leads to an impulse of ~-10^4 kg m^{-1} s^{-1} in one day. Interestingly, the maximum vertical velocities in the model are distributed in patches along the western coast of SMG, a pattern that somewhat resembles the SST distributions observed in the summer of 2008 (Fig. 7). The observation of discontinuous low temperature regions along the coast associated with northerly winds is most likely a consequence of small-scale coastal and bottom configurations, but investigation of such processes is beyond the focus of the present study.

5. Discussion and conclusions

Previous studies have suggested that wind-driven upwelling may occur along the west coast of SMG (Tonini, 2010; Tonini & Palma, 2011; Williams, 2004). Since the wind at this location does not present a well defined seasonality, upwelling events in response to northerly winds must be episodic. Because in-situ observations are scarce and non-systematic, there are no previous reports of upwelling events in this region. Thus, we have relied on remote sensing observations to detect possible upwelling events.

In the present work we have identified the wind conditions required to generate upwelling events on the west coast of SMG, based on their impact on the SST distribution. Our study is primarily based on the analysis of satellite derived SST and wind data. In addition, upwelling events have been characterized by their frequency of occurrence and their characteristic magnitude.

The QuikSCAT wind data is in good agreement with data collected at two coastal stations and an ocean buoy.

According to the adopted criterion, during the warm season we found 56 coastal upwelling-favorable wind events during a 9-year period. During this period evidence of upwelling on SST images was

Table 2
Upwelling events detected during the austral summer 2007–2008. ΔT is the T_{bottom} differences between the time when T_{bottom} starts decreasing until it starts increasing at El Sótano (ES) and Punta Pozos (PP). The wind duration indicates number of days with impulse $<-10^{-4}$ kg m^{-1} s^{-1}. The empty cells indicate that T_{bottom} continues decreasing from the previous event.

Event	Wind		ES		PP	
	Impulse (kg m^{-1} s^{-1})	Duration (days)	ΔT (°C)	Duration (days)	ΔT (°C)	Duration (days)
4 Jan 2008	−10,095	3	−0.96	2	−2.85	2
27 Jan 2008	−10,463	1	−0.37	1	−0.59	3
12 Feb 2008	−14,712	5	−1.49	3	−1.34	2
29 Feb 2008	−10,201	1	−0.98	3	−0.98	3
11 Mar 2008	−10,667	1	−1.21	2	−2.46	5
14 Mar 2008	−12,368	2	−2.24	2		
18 Mar 2008	−13,988	3	−0.59	1	−0.67	1
29 Mar 2008	−10,871	2	−0.08	2	−0.30	2

found on 85% of the events. The estimated volume of upwelled water reaching the sea surface during one relatively intense upwelling event is ~10^{10} m^3 or about 0.6% of the total Gulf volume.

The available in-situ data allowed us to confirm some aspects of the upwelling patterns identified from remote sensing. Bottom mounted temperature records collected near shore provide indirect evidence of upwelling signatures and near simultaneous SST images present surface cooling along the west coast when the northerly wind impulse exceeds a threshold of -10^4 kg m^{-1} s^{-1}. The temperature recorders detected the passage of the bottom front while the SST images revealed the upwelling surface front. However, some of the cooling events detected in bottom mounted temperature recorders are observed when the wind impulse is not large enough to cause surface cooling and are therefore not detected in the satellite derived SST. It should be noted that though the relatively low temporal resolution of QuikSCAT winds (~12 h) could impact on the precise determination of the duration of the upwelling events, comparison with hourly wind data from Puerto Madryn suggests similar durations.

The mean along-shore wind speed observed on the ascending QuikSCAT pass of 7 December 2006 was only about 25% of the mean observed during the descending evening pass. This suggests that the upwelling effectively began some time after the time of the ascending satellite path, and led to the rise of the thermocline and offshore surface flow (Fig. 8b). However, the hydrographic and SST data collected at that time show no evidence of the development of a surface upwelling front. These observations indicate that the upwelling produced by northerly winds will not always manifest at the sea surface.

The wind-impulse required to generate upwelling is more frequently observed in winter than in summer (Fig. 3) but our analysis focused in summer because during that season upwelling may induce readily detectable satellite derived SST anomalies. In contrast, in winter the weak vertical stratification tends to mask the effects of vertical motions on SST. Since theoretical arguments indicate that the impulse required to produce upwelling depends on mixed layer depth and the degree of stratification (Csanady, 1977), which present a strong seasonal signal, it is also expected that the required wind impulse will also have a strong

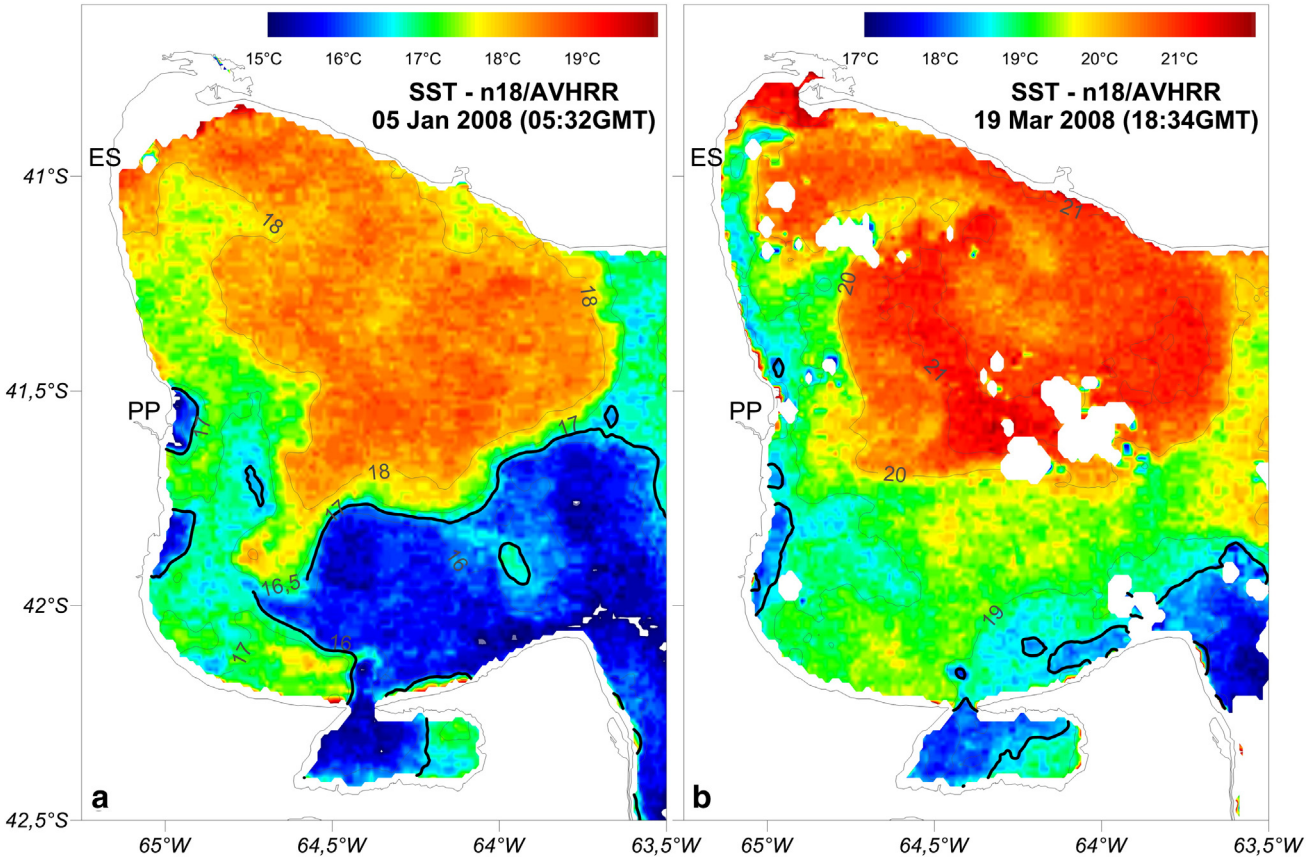

Fig. 7. AVHRR–SST images from (a) 5 January 2008 and (b) 19 March 2008. The heavy black line indicates the 16.5 °C isotherm in (a) and the 18.5 °C in (b).

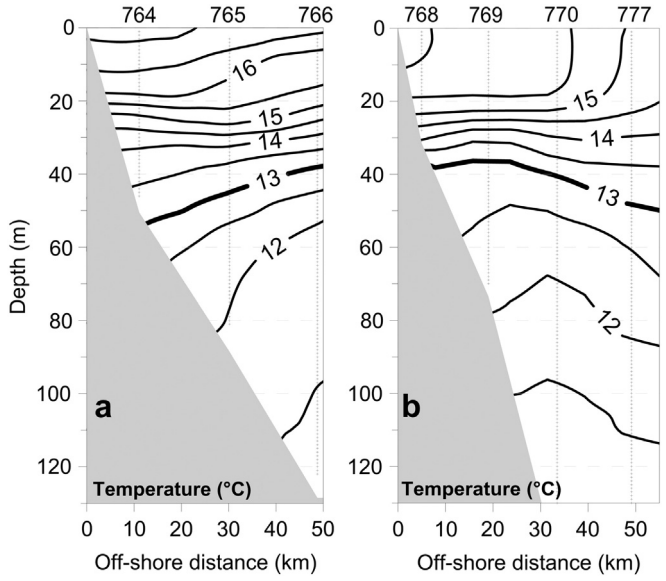

Fig. 8. Vertical temperature sections on the north (a) and south (b) transects occupied in early December 2006 (see Fig. 1 for location). Station numbers are indicated along the top axis.

seasonality. For instance, Haapala (1994) concluded that upwelling of well-mixed waters requires a significantly larger (2–3-fold) wind impulse than in stratified conditions. Furthermore, in winter, when the water column is homogeneous, upwelling may have little or no biological impact, as the nutrient concentration is relatively high throughout the water column.

Upward nutrient fluxes associated with wind induced coastal upwelling frequently lead to growth of phytoplankton. However vertical nutrient fluxes can also be caused by a variety of mechanisms, including enhanced vertical mixing and entrainment. Our search for upwelling evidences was not limited to physical data or to the satellite data period. Observations collected in the western SMG on 3 May 1971 revealed relatively high nitrate concentrations ($NO^{-}_{3} > 2$ μmol/l) throughout the water column (Carreto et al., 1974). In contrast, observations from February 2008 obtained in the same area show nitrate concentrations ($NO^{-}_{2} + NO^{-}_{3}$) of only 0.3 μmol/l, increasing to >2 μmol/l below the seasonal thermocline. These low surface nitrate concentrations are presumably the result of nutrient uptake by phytoplankton during the spring bloom (e.g. Carreto et al., 1995). To determine whether the high near surface nitrates observed in 1971 might be a consequence of coastal upwelling we analyzed wind data from the NCEP reanalysis (Kalnay et al., 1996). Surface wind estimates from two NCEP nodes located near the Gulf indicate southwestern wind of around 10.9 m s^{-1} on 1 and 2 May 1971. In the absence of concurrent temperature data, we speculate that the high nitrate concentration observed in May 1971 was probably associated with an early convection event and not with an upwelling event.

The San Matías Gulf hosts a substantial regional fishery and certain areas have been declared closed to fishing activities. Complementing the scarce in-situ data with remote sensing data is useful to advance our understanding of the processes controlling the regional marine productivity, and to further develop management tools required to sustain the fishing resources.

Acknowledgment

The SST and color images were processed at the Remote Sensing Laboratory of Centro Nacional Patagónico (CENPAT-CONICET) and kindly provided by G. Williams and D.A. Gagliardini. Bottom temperature data were made available by P. Zaidman (CENPAT) and hydrographic data by R. Guerrero (INIDEP). We thank S. Romero for her valuable comments on an earlier draft of this paper. JPP was supported by a Postdoctoral Scholarship provided by CONICET, Argentina. Additional support was provided by grant CRN3070 from the Inter-American Institute for Global Change Research, which is supported by the US National Science Foundation (grant GEO-1128040). Comments from two anonymous reviewers are acknowledged.

References

Acha, E. M., Mianzan, H. W., Guerrero, R. A., Favero, M., & Bava, J. (2004). Marine fronts at the continental shelves of austral South America: Physical and ecological processes. *Journal of Marine Systems*, *44*(1–2), 83–105.

Bakun, A. (1990). Global climate change and intensification of coastal ocean upwelling. *Science, New Series*, *247*(4939), 198–201.

Bava, J., Gagliardini, D. A., Dogliotti, A. I., & Lasta, C. A. (2002). Annual distribution and variability of remotely sensed sea surface temperature fronts in the Southwestern Atlantic Ocean. *29th International Symposium on Remote Sensing of Environment Buenos Aires, Argentina*.

Beardsley, R., Dorman, C., Friehe, A., Rosenfeld, K., & Winnant, C. D. (1987). Local atmospheric forcing during the Coastal Ocean Dynamics Experiment: I. A description of the marine boundary layer and atmospheric conditions over a northern California upwelling region. *Journal of Geophysical Research*, *92*(c2), 1467–1488.

Calvert, S. E., & Price, N. B. (1971). Upwelling and nutrient regeneration in the Benguela Current, October 1968. *Deep Sea Research*, *18*, 505–523.

Carreto, J. I., Lutz, V. A., Carignan, M. O., Colleoni, A. D. C., & Marcos, S. G. D. (1995). Hydrography and chlorophyll-a in a transect from the coast to the shelf-break in the Argentinean Sea. *Continental Shelf Research*, *15*(2–3), 315–336.

Carreto, J. I., Verona, C. A., Casal, A. B., & Laborde, M. A. (1974). Fitoplancton, pigmentos y condiciones ecológicas del Golfo San Matías. *Report*, *10*. (pp. 23–48). Buenos Aires: Instituto de Biología de Mar del Plata.

Castelao, R. M., & Barth, J. A. (2006). Upwelling around Cabo Frio, Brazil: The importance of wind stress curl. *Geophysical Research Letters*, *33*(3), L03602.

Csanady, G. T. (1977). Intermittent 'full' upwelling in Lake Ontario. *Journal of Geophysical Research*, *82*(3), 397–419.

Dellatorre, F. G., Pisoni, J. P., Barón, P. J., & Rivas, A. L. (2012). Tide and wind forced nearshore dynamics in Nuevo Gulf (Northern Patagonia, Argentina): Potential implications for cross-shore transport. *Journal of Marine Systems*, *96–97*, 82–89.

Fennel, W., Radtke, H., Schmidt, M., & Neumann, T. (2010). Transient upwelling in the central Baltic sea. *Continental Shelf Research*, *30*(19), 2015–2026.

Forde, J. J. (2005). *Coastal upwelling along the northern beaches of the North Carolina coast*. IEEE (0-7803-9050-4/05).

Gagliardini, D. A., & Rivas, A. L. (2004). Environmental characteristics of San Matías Gulf obtained from LANDSAT-TM and ETM+ data. *Gayana*, *68*, 186–193.

Garcia, V. M. T., Garcia, C. A. E., Mata, M. M., Pollery, R. C., Piola, A. R., Signorini, S. R., et al. (2008). Environmental factors controlling the phytoplankton blooms at the Patagonia shelf-break in spring. *Deep-Sea Research I*, *55*(9), 1150–1166. http://dx.doi.org/10.1016/j.dsr.2008.04.011.

Glorioso, P. D., & Flather, R. A. (1995). A barotropic model of the currents SE South America. *Journal of Geophysical Research*, *100*(c7), 13427–13440.

González, R., Narvarte, M., & Morsan, E. (2004). Estado de situación de los recursos pesqueros del Golfo San Matías, sus pesquerías, especies asociadas y ambiente: informe ad hoc para la evaluación preliminar de las pesquerías 239 marinas de Río Negro con vistas a la certificación de su sustentabilidad. *Informe Técnico IBMP Nº 03/04* (51 pp.).

Haapala, J. (1994). Upwelling and its influence on nutrient concentration in the coastal area of the Hanko Peninsula, entrance of the Gulf of Finland. *Estuarine, Coastal and Shelf Science*, *38*(5), 507–521.

Kalnay, E., Kanamitsu, M., Kistler, R., Collins, W., Deaven, D., Gandin, L., et al. (1996). The NCEP/NCAR 40-year reanalysis project. *Bulletin of the American Meteorological Society*, *77*(3), 437–471.

Kuo, N. -J., Zheng, Q., & Ho, C. -R. (2000). Satellite observation of upwelling along the western coast of the South China Sea. *Remote Sensing of Environment*, *74*(3), 463–470.

Lentz, S. J., & Chapman, D. C. (2004). The importance of nonlinear cross-shelf momentum flux during wind-driven coastal upwelling. *Journal of Physical Oceanography*, *34*, 2444–2457.

Lucas, A. J., Guerrero, R. A., Mianzan, M. W., Acha, E. M., & Lasta, C. A. (2005). Coastal oceanographic regimes of the Northern Argentine Continental Shelf (34–43°S). *Estuarine, Coastal and Shelf Science*, *65*(3), 405–420.

Lutz, V. A., Segura, V., Dogliotti, A. I., Gagliardini, D. A., Bianchi, A. A., & Balestrini, C. F. (2010). Primary production in the Argentine Sea during spring estimated by field and satellite models. *Journal of Plankton Research*, *32*(2), 181–195.

Matano, R. P., & Palma, E. D. (2008). On the upwelling of downwelling currents. *Journal of Physical Oceanography*, *38*(11), 2482–2500. http://dx.doi.org/10.1175/2008JPO3783.1.

Matano, R. P., Palma, E. D., & Piola, A. R. (2010). The influence of the Brazil and Malvinas Currents on the Southwestern Atlantic Shelf circulation. *Ocean Science Discussion*, *7*, 837–871.

Ocampo-Reinaldo, M., González, R., Williams, G., Storero, L. P., Romero, M. A., Narvarte, M., et al. (2013). Spatial patterns of the Argentine hake *Merluccius hubbsi* and oceanographic processes in a semi-enclosed Patagonian ecosystem. *Marine Biology Research*, *9*(4), 394–406.

Palma, E. D., Matano, R. P., & Piola, A. R. (2004). Three dimensional barotropic response of the southwestern Atlantic shelf circulation to tidal and wind forcing. *Journal of Geophysical Research*, *109*, C08014. http://dx.doi.org/10.1029/2004JC002315.

Palma, E. D., Matano, R. P., & Piola, A. R. (2008). A numerical study of the Southwestern Atlantic Shelf circulation: Stratified ocean response to local and offshore forcing. *Journal of Geophysical Research*, *113*, C11010. http://dx.doi.org/10.1029/2007JC004720.

Park, K. -A., & Kim, K. -R. (2010). Unprecedented coastal upwelling in the East/Japan Sea and linkage to long-term large-scale variations. *Geophysical Research Letters*, *37*, L09603. http://dx.doi.org/10.1029/2009GL042231.

Petrie, B., Topliss, B. J., & Wright, D. G. (1987). Coastal upwelling and eddy development off Nova Scotia. *Journal of Geophysical Research*, *29*(c12), 12979–12991.

Piola, A. R., & Scasso, L. M. (1988). Circulación en el Golfo San Matías. *Geoacta*, *15*(1), 33–51.

Pisoni, J. P. (2012). *Los sistemas frontales y la circulación en las inmediaciones de los Golfos Norpatagónicos.* (Tesis de Doctorado). Argentina: Universidad de Buenos Aires (188 pp., available at http://digital.bl.fcen.uba.ar/Download/Tesis/Tesis_5193_Pisoni.pdf).

Rivas, A. L., Dogliotti, A. I., & Gagliardini, D. A. (2006). Satellite-measured surface chlorophyll variability in the Patagonian shelf. *Continental Shelf Research*, *26*(6), 703–720.

Rivas, A. L., & Pisoni, J. P. (2010). Identification, characteristics and seasonal evolution of surface thermal fronts in the Argentinean Continental Shelf. *Journal of Marine Systems*, *79*(1–2), 134–143.

Romero, S. I., Piola, A. R., Charo, M., & Eiras Garcia, C. A. (2006). Chlorophyll-a variability off Patagonia based on SeaWiFS data. *Journal of Geophysical Research*, *111*(c5), C05021.

Rossi, V., Feng, M., Pattiaratchi, C., Roughan, M., & Waite, A. M. (2013). On the factors influencing the development of sporadic upwelling in the Leeuwin Current system. *Journal of Geophysical Research*, *118*(7), 3608–3621.

Ryther, J. H. (1969). Photosynthesis and fish production in the Sea. *Science, New Series*, *166*(3901), 72–76.

Sabatini, M., & Martos, P. (2002). Mesozooplankton features in a frontal area off northern Patagonia (Argentina) during spring 1995 and 1998. *Scientia Marina*, *66*(3), 215–232.

SMN (1958). *Servicio Meteorológico Nacional.* Estadísticas Climatológicas N° 3, 1941–1950. Buenos Aires, Argentina: Fuerza Aérea Argentina.

SMN (1963). *Servicio Meteorológico Nacional.* Estadísticas Climatológicas N° 6, 1951–1960. Buenos Aires, Argentina: Fuerza Aérea Argentina.

SMN (1981). *Servicio Meteorológico Nacional.* Estadísticas Climatológicas N° 35, 1961–1970. Buenos Aires, Argentina: Fuerza Aérea Argentina.

SMN (1986). *Servicio Meteorológico Nacional.* Estadísticas Climatológicas N° 36, 1971–1980. Buenos Aires, Argentina: Fuerza Aérea Argentina.

Tilburg, C. E. (2003). Across-shelf transport on a continental shelf: Do across-shelf winds matter? *Journal of Physical Oceanography*, *33*(12), 2675–2688.

Tonini, M. H. (2010). *Modelado Numérico del Ecosistema del los Gofos Norpatagónicos.* (Tesis de Doctorado en Ingeniería). Bahía Blanca: Universidad Nacional del Sur (255 pp.).

Tonini, M. H., & Palma, E. D. (2011). Respuesta barotrópica de los golfos norpatagónicos argentinos forzados por mareas y vientos. *Latin American Journal of Aquatic Research*, *39*(3), 481–498.

Tonini, M. H., Palma, E. D., & Piola, A. R. (2013). A numerical study of gyres, thermal fronts and seasonal circulation in austral semi-enclosed gulfs. *Continental Shelf Research*, *65*, 97–110.

Torres, R., Barton, E. D., Miller, P., & Fanjul, E. (2003). Spatial patterns of wind and sea surface temperature in the Galician upwelling region. *Journal of Geophysical Research*, *108*(c4), 3130. http://dx.doi.org/10.1029/2002JC001361.

Williams, G. (2004). *¿Cuáles son las fuentes de nutrientes para mantener la productividad del golfo San Matías?* (Tesis de Licenciatura). Puerto Madryn, Argentina: Universidad Nacional de la Patagonia, San Juan Bosco (100 pp.).

Williams, G., Dogliotti, A. I., Zaidman, P., Solis, M., Narvarte, M., González, R., et al. (2013). Assessment of remotely-sensed sea-surface temperature and chlorophyll-a concentration in San Matías Gulf (Patagonia, Argentina). *Continental Shelf Research*, *52*, 159–171.

Wood, J. E., Roughan, M., & Tate, P. (2012). Finding a proxy for wind stress over the coastal ocean. *Marine and Freshwater Research*, *63*(6), 528–544.